Magnetic moments in a helical edge can make weak correlations seem strong

Jukka I. Väyrynen, Florian Geissler, and Leonid I. Glazman

Phys. Rev. B **93**, 241301 — Published 10 June 2016

DOI: 10.1103/PhysRevB.93.241301

Magnetic moments in a helical edge can make weak correlations seem strong

Jukka I. Väyrynen,[1] Florian Geissler,[2] and Leonid I. Glazman[1]

[1] *Department of Physics, Yale University, New Haven, CT 06520, USA*
[2] *Institute for Theoretical Physics and Astrophysics, University of Würzburg, 97074 Würzburg, Germany*

We study the effect of localized magnetic moments on the conductance of a helical edge. Interaction with a local moment is an effective backscattering mechanism for the edge electrons. We evaluate the resulting differential conductance as a function of temperature T and applied bias V for any value of V/T. Backscattering off magnetic moments, combined with the weak repulsion between the edge electrons results in a power-law temperature and voltage dependence of the conductance; the corresponding small positive exponent is indicative of insulating behavior. Local moments may naturally appear due to charge disorder in a narrow-gap semiconductor. Our results provide an alternative interpretation of the recent experiment by Li et al.[1] where a power-law suppression of the conductance was attributed to strong electron repulsion within the edge, with the value of Luttinger liquid parameter K fine-tuned close to 1/4.

Introduction - In search for topological insulators, the III-V semiconductor structures with band inversion appeared as a viable option[2]. The band inversion does occur in the type-2 heterostructure, InAs/GaSb. If the layers forming the well are narrow enough, the hybridization of states across the interface results in a formation of a gap; in the "topological" phase, the gap is accompanied by edge states free from elastic backscattering. These putative states became a target of an extensive set of measurements[1,3–6]. First, a surprisingly robust conductance quantization was found[5]. A later experiment[1] explained the temperature-independent quantized conductance G as an inadvertent deviation from the linear-response regime. The observed[1] power-law temperature and bias voltage dependence of the differential conductance was suggestive of insulating behavior. Assuming topologically protected edge states, it can be interpreted as a manifestation of strong-interaction physics: at low energies, even a single impurity can "cut" the edge, suppressing charge transport[7] if the Luttinger parameter is very small, $K < 1/4$[8,9] ($K = 1$ corresponds to non-interacting electrons). Measurements[1] yield $K \approx 0.22$ (with a 5% error), which is very close to the critical value of 1/4; an increase of K by mere 12% would change the sign of dG/dT. Fine-tuning K to such a stable value seems improbable, given the dependence of the edge state velocity on the gate voltages, varied in the experiment. The reliance on fine-tuning in the current explanation of experiments provides an impetus to search for alternatives less sensitive to a specific value of K.

We find that scattering off localized magnetic moments may lead to temperature and bias dependences of the differential conductance similar to those observed[1] at moderately weak interaction, $K \approx 0.8$, without fine-tuning of K. The origin of localized moments in InAs/GaSb quantum wells is not known, but the narrow 40-60K gap in these systems may allow for the presence of charge puddles[10] which can act as magnetic impurities[11]. In the present work we focus on the non-linear current-voltage characteristics and on the effects of electron-electron interactions within the helical edge which were not considered in Ref.[11].

The setup and qualitative description of the main results - We start by considering a single spin-1/2 magnetic moment $\mathbf{S}$ coupled to a helical edge. The isolated edge is described[8] by a Luttinger liquid Hamiltonian H_0; the local moment is coupled to the edge electrons by, generally, anisotropic exchange interaction. Separating out its isotropic part, the full time-reversal symmetric Hamiltonian of the coupled edge-impurity system can be written as

$$H = H_{\rm iso} + \sum_{ij} \delta J_{ij} S_i s_j(x_0) \tag{1}$$

with $H_{\rm iso}$ being the Hamiltonian with isotropic exchange:

$$H_{\rm iso} = H_0 + J_0 \mathbf{S}\cdot\mathbf{s}(x_0) \tag{2}$$

Here, $\mathbf{S}$ is the spin-1/2 impurity spin operator, and $\mathbf{s}(x_0) = \frac{1}{2}\sum_{\alpha\beta}\psi^\dagger_\alpha(x_0)\boldsymbol{\sigma}_{\alpha\beta}\psi_\beta(x_0)$ is the edge electron spin density at the position x_0 of the contact interaction with the local moment. (From hereon we will omit the position arguments.) We shall assume $\delta J_{ij} \ll J_0$ so that the exchange is almost isotropic[11]. Thus we can treat the second term in Eq. (1) as a perturbation.

The first term in $H_{\rm iso}$, Eq. (2) is the bosonized Luttinger-liquid Hamiltonian describing the interacting helical edge electrons, $H_0 = (2\pi)^{-1} v \int dx[\Pi^2 + (\partial_x\varphi)^2]$; we assume the dimensionless exchange coupling parameter to be small, $\rho J_0 \ll 1$ (here ρ is the electron density of states per spin per unit edge length). The bosonic fields commute as $[\varphi(x), \Pi(y)] = i\pi\delta(x-y)$. We have rescaled the fields by appropriate factors of $\sqrt{K}$; the bosonization identity is $\psi_\beta(x) = (2\pi a)^{-1/2} e^{-i(\beta\sqrt{K}\varphi - \frac{1}{\sqrt{K}}\int_{-\infty}^{x} dx'\Pi)}$ with $\beta = +/-$ for right/left movers (or spin up/down; we take $\mathbf{z}$-axis to be the spin quantization axis of helical electrons at Fermi energy); a is the short-distance cutoff. In bosonic representation, the spin density takes form $s_x \pm i s_y = \pm i(2\pi a)^{-1} e^{\pm 2i\sqrt{K}\varphi}$, $s_z = \frac{1}{2\pi\sqrt{K}}\Pi$. Using it,

we re-write the exchange interaction Hamiltonian as

$$J_0\mathbf{S}\cdot\mathbf{s}\to J_\perp\frac{-i}{4\pi a}(S_+e^{-2i\sqrt{K}\varphi}-S_-e^{2i\sqrt{K}\varphi})+J_z\frac{1}{2\pi\sqrt{K}}S_z\Pi\,. \tag{3}$$

Even though the bare Hamiltonian (2) is isotropic, $J_\perp = J_z = J_0$, the exchange becomes anisotropic under renormalization group (RG) flow, as the scaling dimensions of the corresponding spin densities in Eq. (3), $\Delta_\perp = K$ and $\Delta_z = 1$, differ from each other[12], see also Eqs.(4)–(5) below. The isotropy breaking is not an artefact: anisotropy is already present in the bare Hamiltonian even at $K = 1$ due to the spin-orbit interaction; the Hamiltonian has no SU(2) symmetry but only a smaller U(1) symmetry (spin rotations about z-axis).

The weak-coupling ($\rho J \ll 1$ and $1-K \ll 1$) RG equations for $J_\perp$ and J_z are[13–15] (here E is the running cutoff)

$$\frac{dJ_\perp}{d\ln E} = -(1-K)J_\perp - \rho J_z J_\perp \tag{4}$$

$$\frac{dJ_z}{d\ln E} = -\rho J_\perp^2 \tag{5}$$

The right-hand-side of the first equation starts at tree level with a coefficient[12,16] $1-\Delta_\perp = 1-K$; the second equation does not have such a term since $\Delta_z = 1$. The terms second-order in J are due to the Kondo effect and can be derived from poor man scaling[17], or from an operator product expansion[12,16].

Starting from isotropic initial condition, $J_0 > 0$, Eq. (4) shows that there are two regimes of parameters: $\rho J_0 \ll 1-K$ and $\rho J_0 \gg 1-K$. In the latter case $1-K$ can be dropped from Eq. (4), and the physics is similar to that of the case $K = 1$[11].

In this paper we focus on the opposite limit, $\rho J_0 \ll 1-K$. (Note, such initial condition can be satisfied even if the electron-electron interaction is weak, $1-K \ll 1$.) In this case the RG flow governed by Eqs. (4)–(5) can be divided into two regimes separated by energy scale T^* (we use units $k_B = \hbar = 1$) defined by the crossover condition[18] $\rho J_z(T^*) = 1-K$,

$$T^* = D(\frac{1}{\sqrt{2}}\frac{\rho J_0}{1-K})^{1/(1-K)}\,. \tag{6}$$

Here $D \sim E_g$ is the bare cutoff which we take to be the bulk band gap[19]. At energies $E \gg T^*$ one can ignore $\rho J_z(E)$ in (4), whereas at $E \ll T^*$ one can ignore $1-K$. Next, we discuss electron backscattering in the high energy limit, $E \gg T^*$ where interaction ($K \neq 1$) is important.

The backscattering current at energies above T^* - The isotropic exchange Hamiltonian (2) alone does not backscatter edge electrons in steady state (DC bias) since each backscattering event is accompanied by an action of the nilpotent operator S_- on the impurity spin polarized along $\mathbf{z}$-axis[20]. The presence of anisotropy in the exchange, Eq. (1), gives rise to backscattering. This perturbation in Eq. (1) can be treated using Fermi Golden Rule, assuming equilibrium impurity polarization $\langle\mathbf{S}\rangle = \mathbf{z}\frac{1}{2}\tanh\frac{eV}{2T}$[21]. Integration over electron phase space volume leads to a backscattering current $\langle\delta I\rangle \sim e^2V(\rho\delta J)^2$. We can find the full temperature and bias voltage dependence by solving for the renormalized coupling δJ. Since the pertinent constant δJ couples to the spin-flip operators $e^{\pm 2i\sqrt{K}\varphi}$, it acquires a power-law energy dependence $\delta J(E) = (D/E)^{1-K}\delta J(D)$ for $E > T^*$. Taking $E \sim \max(T, eV)$, the T and V -dependent backscattering current becomes (valid at $\max(T, eV) \gg T^*$)

$$\langle\delta I\rangle = \frac{e^2}{h}cV\,T^{-2(1-K)}[\max(1, eV/T)]^{-2(1-K)}\,, \tag{7}$$

where constant c depends on the bare exchange tensor. Equation (7) is a simplified version of our main result. Its detailed version, see Eq. (14), reveals, in addition to $eV/T \sim 1$, yet another crossover in the current-voltage characteristic occurring at $\frac{eV}{T} \sim \rho J \ll 1$; it is associated with the details of impurity spin torque and relaxation, ignored in Eq. (7).

Long edge conductance at energies above T^* - Let us now consider a long sample which may host many impurities near the edge. A single impurity contributes an amount $\delta R \approx \delta G/G_0^2$to the edge resistance (here $G_0 = e^2/h$ and $\delta G = d\langle\delta I\rangle/dV$). In a long sample with N impurities we can simply add resistances if the impurities are dilute enough[22]. The impurities dominate the edge resistance if $N\delta G \gg G_0$, where the same typical value δG for each impurity is used. In this case one finds $G \approx G_0^2/N\delta G$ for the conductance of a single edge. Here δG is evaluated with the help of Eq. (14) or its simplified version, Eq. (7), both valid at $\max(T, eV) > T^*$.

Using Eq. (7) one finds a power-law dependence $G(V,T) \approx (G_0/cN)[\max(T, eV)]^{2(1-K)}$. In Ref.[1] the authors found a fit $G \propto V^{0.37}$ in the regime $eV > T$ for a sample of length $L = 1.2\mu$m (see inset in Fig. 4 of Ref.[1]). Matching with our theory of many impurities leads to $2(1-K) \approx 0.37$, or $K \approx 0.82$. Thus, in presence of many impurities, even moderately weak interactions can give rise to the power law seen in Ref.[1]. The two possible explanations (many impurities and weak interaction *vs.* single impurity and strong interaction) of the observed conductance predict different dependencies of G on the edge length: for many impurities one expects $N \propto L$ and hence resistive behavior $G \propto L^{-1}$. Although $G(L)$ dependence is not reported in Ref.[1], the earlier work[5] found it to be linear at $L \gtrsim 10\mu$m [23]. The presence of magnetic impurities may also be identified from their subtle effect on the non-linear I-V characteristics, which we discuss next.

Refinement of Eq. (7) - The simplified form Eq. (7) of the current-voltage characteristic misses several fine points relevant for the future analysis of experiments: (1) it does not provide the accurate form of the crossover at $eV/T \sim 1$, and (2) it does not reveal an additional crossover at smaller bias, $eV/T \sim \rho J$. The latter crossover is associated with the precession of the local magnetic moment in the exchange field $h \sim eV\rho J$ pro-

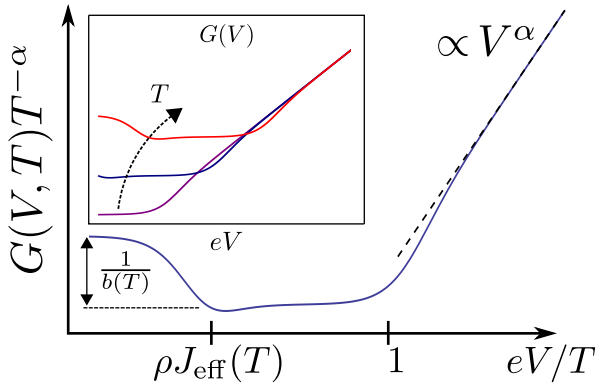

FIG. 1. (Color online) Log-log plot of the scaled conductance, $G\cdot T^{-\alpha}$, in the presence of many impurities, $G\propto 1/\delta G$. Here $\delta G = d\langle\delta I\rangle/dV$ and $\alpha = 2-2K > 0$ are taken from Eq. (14), valid at intermediate energies $\max(T,eV) > T^*$. The conductance has two crossover scales in its V-dependence. The higher crossover is at $eV\sim T$: above it, conductance increases (upon increasing V) asymptotically as a power law with exponent $\alpha>0$ (dashed line). Below it, G stays roughly constant until the lower crossover scale, $eV\sim\rho J_{\rm eff}(T)T$, is reached. Below it, the conductance changes by a factor $1/b(T)>1$ that depends weakly on temperature, see discussion below Eq. (16). The inset shows $G(V)$ at three different temperatures T (increasing from the lowest to highest curve).

duced by the spins of itinerant edge electrons under a finite bias[21]. The crossover occurs once the precession frequency $\propto h$ becomes comparable to the Korringa relaxation rate,[24] $1/\tau_K\sim(\rho J)^2T$, as we will see in a detailed derivation of backscattering current.

The current operator of backscattered electrons is given by[25] $\delta I=-e\partial_t\delta N$ where $2\delta N=(N_L-N_R)$ is the difference between the number of left and right movers on the edge; it obeys $[\delta N,\, s_i(x_0)]=i\epsilon_{zin}s_n(x_0)$ and commutes with H_0. The decomposition (1) of the Hamiltonian is useful because at zero frequency the Hamiltonian $H_{\rm iso}$, Eq. (2), does not lead to backscattering of helical edge electrons[20]. It can be seen by noticing that: (i) $\partial_t\langle S_z\rangle=0$ in a steady state, because S_z is bounded; this allows one to write the average backscattering current as[11] $\langle\delta I\rangle=-e\partial_t\langle S_z^{tot}\rangle$ with $S_z^{tot}=\delta N+S_z$, and (ii) the operator S_z^{tot} commutes with $H_{\rm iso}$ and therefore is a conserved quantity in absence of δJ_{ij}. Hence $\partial_t\langle S_z^{tot}\rangle|_{\delta J\to0}=0$ and $\langle\delta I\rangle|_{\delta J\to0}=0$. We focus here on the case of a single magnetic moment; in the presence of many moments, we can define $S_z^{tot}=\delta N+\sum_n S_z^{(n)}$ where the sum is over the localized spins $\mathbf{S}^{(n)}$. In this work, we ignore the effects of correlations between the localized spins and coherent backscattering, allowing us to simply add up single-moment contributions to the edge resistance. This is justified for dilute spins, as discussed in more detail in Ref.[22].

From hereon, we consider scattering off a single spin, and express the average steady-state backscattered current as $\langle\delta I\rangle=-e\partial_t\langle S_z^{tot}\rangle$. Commuting with the Hamiltonian (1) leads to [we denote $\delta J_{++}=\delta J_{xx}-\delta J_{yy}+i(\delta J_{xy}+\delta J_{yx})$, $S_\pm=S_x\pm iS_y$ for brevity]

$$\langle\delta I\rangle = e\sum_{i,j=x,y}\epsilon_{ijz}\left(\delta J_{jz}\langle S_i:s_z:\rangle+\delta J_{zj}\langle S_z:s_i:\rangle\right)$$
$$+e{\rm Im}\delta J_{++}\langle S_-:s_-:\rangle+\frac{1}{2}\rho e^2V\left(\delta J_{yz}\langle S_x\rangle-\delta J_{xz}\langle S_y\rangle\right). \tag{8}$$

In agreement with the presence of an integral of motion, the average current vanishes when $\delta J\to0$. The averaging above is done with respect to the density matrix ϱ with Hamiltonian (1) in presence of a finite bias voltage, $\varrho\sim e^{-\beta\left(H-eVS_z^{tot}\right)11}$. We denote $:s_j:=s_j-\langle s_j\rangle_0$ with $\langle\rangle_0$ being the thermal average in absence of exchange interaction, $\varrho_0\sim e^{-\beta(H_0-eV\delta N)}$. The last term in (8) comes from the reducible part $\langle s_j\rangle_0=\frac{1}{2}\delta_{jz}\rho eV$.

Equation (8) is evaluated at time t long enough so that the steady-state value of $\langle\mathbf{S}\rangle$ has been reached. The averages $\langle S_k:s_l:\rangle$ can be evaluated approximately in the exchange interaction assuming a separation of time scales for the itinerant electron and spin dynamics[22]. The approximation results in

$$\langle S_k:s_l:\rangle(t)\approx-\sum_j(\delta_{kj}J_0+\delta J_{kj})\frac{1}{2}{\rm Im}C_{jl}$$
$$-\sum_{ijn}(\delta_{ij}J_0+\delta J_{ij})\epsilon_{ikn}\langle S_n\rangle\,{\rm Re}C_{jl}\,. \tag{9}$$

Here $\langle S_n\rangle$ is the steady-state impurity spin polarization created by the current passing on the edge. The integrated correlation function $C_{nl}=\int_0^\infty dt'\,\langle s_n(0):s_l(t'):\rangle_0$ depends on temperature and bias voltage (through the average $\langle\ldots\rangle_0$). The only non-zero components of the matrix of C_{nl} are the diagonals and $C_{xy}=-C_{yx}\neq0$, the latter being due to finite bias voltage. The temperature and bias dependence of C_{nl} appearing in Eq. (9) can be moved into the T and V dependence of running couplings $J_{ij}(T,V)$[22]. Inserting Eq. (9) into Eq. (8) allows us to express the backscattering current in terms of the running couplings and steady-state values of the local-moment spin polarization $\langle\mathbf{S}\rangle$, see Ref.[22]. The last is found from the Bloch equations[26]. At $\delta J=0$, its only finite component is $\langle S_z\rangle=\frac{1}{2}\tanh\frac{eV}{2T}$ due to the $U(1)$ symmetry. Aiming at the lowest-order in δJ result for $\langle\delta I\rangle$, we need to find $\langle S_{x,y}\rangle$ to the first order in δJ. Unlike $\langle S_z\rangle$, which is a function of eV/T given by thermodynamics, the components $\langle S_{x,y}\rangle$ depend[22] on both the effective field $h_z=\frac{1}{2}eV\rho J_z$ generated by the bias voltage, and on the local-moment Korringa relaxation rate $\tau_K^{-1}=\frac{\pi}{2}\rho^2(J_\perp^2\frac{\frac{eV}{2T}}{\tanh\frac{eV}{2T}}+J_z^2)T$. (We use here the running couplings with their implicit dependence on V and T.) The backscattering current is

$$\langle\delta I\rangle=e\frac{\pi}{4}eV\rho^2|\delta J_{++}(T,V)|^2+e\frac{\pi}{4}eV\frac{1}{2}R(T,V)$$
$$\times\sum_{i=x,y}\rho^2\left(\delta J_{zi}(T,V)+\frac{J_\perp(T,V)}{J_z(T,V)}\delta J_{iz}(T,V)\right)^2. \tag{10}$$

Here the first term arises from non-zero $\langle S_z\rangle$ and can be derived simply from Fermi Golden Rule by assuming $\langle \mathbf{S}\rangle = \mathbf{z}\frac{1}{2}\tanh\frac{eV}{2T}$. In the second term, function

$$R(T,V) \approx \frac{\frac{J_z(T,0)}{J_{\rm eff}(T)} + x^2}{1+x^2}\,, \quad x = \frac{eV}{2T}\frac{2/\pi}{\rho J_{\rm eff}(T)}\,, \qquad (11)$$

comes from $\langle S_{x,y}\rangle \neq 0$ and therefore depends on the ratio $h_z/\tau_K = x$. Here we abbreviated $\rho J_{\rm eff}(T) = \rho[J_\perp(T,0)^2 + J_z(T,0)^2]/J_z(T,0) \ll 1$. In Eq. (11) the term $J_z/J_{\rm eff} \lesssim 1$ only matters at very small bias $eV \ll T\rho J_{\rm eff} \ll T$; thus we have neglected the V-dependence in it.

In Eq. (10) the current is written in terms of the running couplings $J_{ij}(T,\, V)$. Next, we will write it in terms of the bare couplings, which allows us to see explicitly the T, V-dependence of $\langle \delta I\rangle$. At $T^* < \max(eV,\, T) < D$ one has[22]

$$X(T,V) \approx X(D)\left(\frac{D}{2\pi T}\right)^{1-K}\sqrt{F(\frac{eV}{2T})} \qquad (12)$$

with a function

$$F(y) = KB(K+i\frac{y}{\pi}, K-i\frac{y}{\pi})\frac{\sinh y}{y} \approx \frac{B(K,K)}{[1+A(K)y^2]^{1-K}}\,. \qquad (13)$$

Here $A(K) = \pi^{-2}\Gamma(K)^{\frac{2}{1-K}}$ and B is the Euler Beta function; X stands for any of the quantities, ${\rm Re}\delta J_{++}$, ${\rm Im}\delta J_{++}$, and $\delta J_{zi} + \frac{J_\perp}{J_z}\delta J_{iz}$ $(i = x,\, y)$, which appear in Eq. (10).

Using Eqs. (10)–(13) we arrive at the central result of this paper: the temperature and bias dependence of the current can be lumped in a product of several simple terms,

$$\langle \delta I\rangle = \delta G_0\left[\frac{D}{2\pi T}\right]^{2-2K} V\frac{B(K,K)}{[1+A(K)(\frac{eV}{2T})^2]^{1-K}} f(x,T)\,,$$
$$f(x,T) = \frac{b(T)+x^2}{1+x^2}\,,\; x = \frac{eV}{2T}\frac{2/\pi}{\rho J_{\rm eff}(T)}. \qquad (14)$$

Here the T-independent factor is $\delta G_0 = \frac{e^2}{\hbar}\frac{\pi}{4}\rho^2\delta J_{\rm tot}^2(D)\,,$

$$\delta J_{\rm tot}^2(D) = |\delta J_{++}(D)|^2 + \frac{1}{2}\sum_{i=x,y}[\delta J_{zi}(D) + \delta J_{iz}(D)]^2\,, \qquad (15)$$

while $J_{\rm eff}(T)$ and

$$b(T) = 1 - \frac{(1-\frac{J_z(T,0)}{J_{\rm eff}(T)})\frac{1}{2}\sum_{i=x,y}[\delta J_{zi}(D) + \delta J_{iz}(D)]^2}{|\delta J_{++}(D)|^2 + \frac{1}{2}\sum_{i=x,y}[\delta J_{zi}(D) + \delta J_{iz}(D)]^2} \qquad (16)$$

display a weak temperature dependence[22]. (For typical values of exchange couplings $\delta J_{ij}(D)$ function $b(T)$ can be well approximated by a constant of order 1: $0.67 \leq b(T) \leq 0.83$ in the interval $T^* \leq T \leq D$[22].) At a fixed temperature T, the current dependence on bias V has two well-separated crossover scales described by the last two factors in (14). The smaller scale, $V \sim T\rho J_{\rm eff}(T)$, is associated with the impurity spin dynamics. The crossover at the higher scale, $V \sim T$, occurs between the linear and weakly-nonlinear $\langle \delta I\rangle$ vs. V dependencies. Near this crossover one may set $f \to 1$ in Eq. (14), reproducing the result of Eq. (7) with, however, accurate crossover behavior near $eV \sim T$.

The backscattering current at energies below T^* - At energies $E \lesssim T^*$, one may neglect the small term $\propto (1-K)$ in (4)–(5) and consider the resulting weak-coupling Kondo RG with the initial condition $\rho J_\perp(T^*) = \sqrt{2}(1-K)$[22]. For small $1-K$, it yields the Kondo temperature $T_K \sim T^* e^{-1/\sqrt{2}(1-K)} \ll T^*$. The RG flow erases the uniaxial anisotropy created by $K \neq 1$, and $J_z \approx J_\perp$ at energies below T^*. As a result, $J_{\rm eff} = 2J_z$ in Eq. (11) and $R = (\frac{1}{2} + x^2)/(1+x^2)$. Similarly, the anisotropic perturbation in Eq. (1) becomes RG-irrelevant, and Eq. (12) is replaced[11] by $X(E) \approx X(T^*)\frac{\ln E/T_K}{\ln T^*/T_K}$. Hence, the backscattering current becomes

$$\langle \delta I\rangle = \delta G_0 V\left[\frac{\ln\max(T, eV)/T_K}{\ln T^*/T_K}\right]^2\frac{b+x^2}{1+x^2}\,, \qquad (17)$$

valid for $T_K < \max(T, eV) < T^*$. Here b is given by Eq. (16) which becomes independent of T upon setting $J_{\rm eff} = 2J_z$. Similarly, δG_0 was introduced below Eq. (14) but now one must use $\delta J_{\rm tot}^2(T^*)$ in it with the "new" bare cutoff.

The coupling constant $\rho J_z(E) \sim [\ln(E/T_K)]^{-1}$ grows in the course of RG, and below the Kondo temperature, $\max(T, eV) < T_K$, Eqs. (4)–(5) are no longer valid. In this regime one can use the phenomenological local-interaction Hamiltonian[27,28] to obtain $\delta G(V,T) \propto T^4 g(V/T)$; the crossover function $g(x)$ has asymptotes $g(x \to 0) = {\rm const}$ and $g(x \gg 1) \sim x^4$. Details can be found in Ref.[28] upon setting $K = 1$ therein. Note that δG decreases when reducing T, eV and thus leads to $G = e^2/h$ in the limit of zero temperature and bias. This behavior is opposite from Eq. (14) which indicated an insulating edge at low energies.

Conclusions - We analyzed the joint effect of two weak interactions on the edge conduction in a 2D topological insulator. These interactions are: the repulsion between itinerant electrons of an edge state, and their exchange with the local magnetic moments. This joint effect may result in a seemingly insulating behavior of the edge conduction down to a low temperature scale T^*, see Eq. (6): at $\max(T, eV) \gtrsim T^*$, the single-impurity backscattering current $\langle \delta I\rangle$ *grows* as a power law upon lowering temperature or bias, see Eq. (14), or Fig. 1 for the conductance in presence of many moments. Localized magnetic moments may appear in a narrow-gap semiconductor as a consequence of charge disorder[11]. Scattering off magnetic moments provides an alternative explanation of the recent experiment[1], assuming T^* is below the temperature range explored in[1]. [None of the considered interactions break the time-reversal symmetry[29], so at low energies, $\max(T, eV) \ll T^*$, backscattering is suppressed,

see Eq. (17).] The developed theory is also applicable to magnetically-doped[30,31] heterostructures. Finally, we find two crossovers in the I-V characteristics: the main one occurs at $eV \sim T$; a more subtle one occurs at lower bias, $eV \sim \rho JT$, see Fig. 1. Its observation in future experiments may provide evidence for the considered mechanism of the edge state excess resistance.

ACKNOWLEDGMENTS

We thank Richard Brierley, Rui-Rui Du, and Hendrik Meier for discussions. This work was supported by NSF DMR Grant No. 1206612 and DFG through SFB 1170 "ToCoTronics".

[1] T. Li, P. Wang, H. Fu, L. Du, K. A. Schreiber, X. Mu, X. Liu, G. Sullivan, G. A. Csáthy, X. Lin, and R.-R. Du, Phys. Rev. Lett. **115**, 136804 (2015).
[2] C. Liu, T. L. Hughes, X.-L. Qi, K. Wang, and S.-C. Zhang, Phys. Rev. Lett. **100**, 236601 (2008).
[3] I. Knez, C. T. Rettner, S.-H. Yang, S. S. P. Parkin, L. Du, R.-R. Du, and G. Sullivan, Phys. Rev. Lett. **112**, 026602 (2014).
[4] E. M. Spanton, K. C. Nowack, L. Du, G. Sullivan, R.-R. Du, and K. A. Moler, Phys. Rev. Lett. **113**, 026804 (2014).
[5] L. Du, I. Knez, G. Sullivan, and R.-R. Du, Phys. Rev. Lett. **114**, 096802 (2015).
[6] F. Nichele, H. J. Suominen, M. Kjaergaard, C. M. Marcus, E. Sajadi, J. A. Folk, F. Qu, A. J. A. Beukman, F. K. de Vries, J. van Veen, S. Nadj-Perge, L. P. Kouwenhoven, B.-M. Nguyen, A. A. Kiselev, W. Yi, M. Sokolich, M. J. Manfra, E. M. Spanton, and K. A. Moler, ArXiv e-prints (2015), arXiv:1511.01728 [cond-mat.mes-hall].
[7] C. L. Kane and M. P. A. Fisher, Phys. Rev. Lett. **68**, 1220 (1992).
[8] C. Wu, B. A. Bernevig, and S.-C. Zhang, Phys. Rev. Lett. **96**, 106401 (2006).
[9] C. Xu and J. E. Moore, Phys. Rev. B **73**, 045322 (2006).
[10] J. I. Väyrynen, M. Goldstein, and L. I. Glazman, Phys. Rev. Lett. **110**, 216402 (2013).
[11] J. I. Väyrynen, M. Goldstein, Y. Gefen, and L. I. Glazman, Phys. Rev. B **90**, 115309 (2014).
[12] D. Sénéchal, in *Theoretical Methods for Strongly Correlated Electrons*, CRM Series in Mathematical Physics, edited by D. Sénéchal, A.-M. Tremblay, and C. Bourbonnais (Springer New York, 2004) pp. 139–186.
[13] D.-H. Lee and J. Toner, Phys. Rev. Lett. **69**, 3378 (1992).
[14] A. Furusaki and N. Nagaosa, Phys. Rev. Lett. **72**, 892 (1994).
[15] J. Maciejko, C. Liu, Y. Oreg, X.-L. Qi, C. Wu, and S.-C. Zhang, Phys. Rev. Lett. **102**, 256803 (2009).
[16] J. Cardy, *Scaling and renormalization in statistical physics*, Vol. 5 (Cambridge university press, 1996).
[17] P. Anderson, Journal of Physics C: Solid State Physics **3**, 2436 (1970).
[18] T. Giamarchi, *Quantum Physics in One Dimension*, International Series of Monographs on Physics (Clarendon Press, 2003).
[19] In general, the cutoff depends on the microscopic structure of the impurity. If the exchange term in Eq. (1) originates from a charge puddle, the cutoff is $D \sim \min(E_g, E_C, \delta)$, where E_C and δ are, respectively, the energies of charged and chargeless excitations in a puddle[11].
[20] Y. Tanaka, A. Furusaki, and K. A. Matveev, Phys. Rev. Lett. **106**, 236402 (2011).
[21] The bias voltage creates an imbalance between left and right movers and a non-zero $\langle s_z \rangle$ in Eq. (2). This results in non-zero $\langle S_z \rangle$ through the exchange interaction (2).
[22] See Supplemental Material for details. The supplement includes references to[32–38].
[23] Recently, in the topologically trivial regime (but still edge-dominated) $G \propto L^{-1}$ has been observed even at submicron lengths[6].
[24] J. Korringa, Physica **16**, 601 (1950).
[25] C. L. Kane and M. P. A. Fisher, Phys. Rev. Lett. **72**, 724 (1994).
[26] F. Bloch, Phys. Rev. **70**, 460 (1946).
[27] T. L. Schmidt, S. Rachel, F. von Oppen, and L. I. Glazman, Phys. Rev. Lett. **108**, 156402 (2012).
[28] N. Lezmy, Y. Oreg, and M. Berkooz, Phys. Rev. B **85**, 235304 (2012).
[29] We disregard here the possibility of spontaneous symmetry breaking[39,40].
[30] T. Jungwirth, J. Sinova, J. Mašek, J. Kučera, and A. H. MacDonald, Rev. Mod. Phys. **78**, 809 (2006).
[31] We expect $T^* \sim 0.9$mK for a Mn-doped InAs-based heterostructure[41]. To arrive at this estimate we used the following parameters: exchange coupling $J/a_0^3 \sim 1eV$ per unit cell volume[41], lattice constant $a_0 \approx 0.6$nm, quantum well thickness $d \approx 11.5$nm, edge state velocity $v \approx 5.7 \times 10^4$m/s, penetration depth $\xi \approx 16$nm, $E_g \approx 54$K[1], and $K \approx 0.8$.
[32] H.-P. Breuer and F. Petruccione, *The theory of open quantum systems* (Oxford University Press on Demand, 2002).
[33] I. Gradshteyn, I. Ryzhik, and A. Jeffrey, *Table of Integrals, Series and Products 5th edn (New York: Academic)* (1994).
[34] T. Giamarchi and H. J. Schulz, Phys. Rev. B **37**, 325 (1988).
[35] I. V. Gornyi, A. D. Mirlin, and D. G. Polyakov, Phys. Rev. Lett. **95**, 046404 (2005).
[36] M. Dyakonov, Solid State Communications **92**, 711 (1994).
[37] J. Maciejko, Phys. Rev. B **85**, 245108 (2012).
[38] E. Eriksson, Phys. Rev. B **87**, 235414 (2013).
[39] B. L. Altshuler, I. L. Aleiner, and V. I. Yudson, Phys. Rev. Lett. **111**, 086401 (2013).
[40] O. M. Yevtushenko, A. Wugalter, V. I. Yudson, and B. L. Altshuler, EPL (Europhysics Letters) **112**, 57003 (2015).
[41] Q.-Z. Wang, X. Liu, H.-J. Zhang, N. Samarth, S.-C. Zhang, and C.-X. Liu, Phys. Rev. Lett. **113**, 147201 (2014).